Sensors and Actuators B 244 (2017) 577–584

Contents lists available at ScienceDirect

Sensors and Actuators B: Chemical

journal homepage: www.elsevier.com/locate/snb

Supramolecular complex based on MWNTs/Boltorn H40 provides fast response to a Sandwich-type amperometric lactate biosensor

Marcelo R. Romero [a], Damián Peralta [a], Cecilia I. Alvarez Igarzabal [a], Ana M. Baruzzi [b], Miriam C. Strumia [a,*], Fernando Garay [b,*]

[a] IMBIV-CONICET. Dpto. de Química Orgánica, Facultad de Ciencias Químicas, Universidad Nacional de Córdoba, 5000 Córdoba, Argentina
[b] INFIQC-CONICET, Dpto. de Físico Química, Facultad de Ciencias Químicas, Universidad Nacional de Córdoba, 5000 Córdoba, Argentina

ARTICLE INFO

Article history:
Received 11 September 2016
Received in revised form
30 November 2016
Accepted 2 January 2017
Available online 5 January 2017

Keywords:
Self-assembled
Sandwich-type biosensor
Lactate
Nanotube
Hydrogel
Hyperbranched

ABSTRACT

Most sandwich-type biosensors can be used several times, since their long-time stability generally ranges from weeks to several months. However, the response-time of this kind of sensors is typically slow because reagents and products have to diffuse through filtering membranes and the enzymatic matrix. In this manuscript, multiwalled carbon nanotubes (MWNTs) have been used for wiring the enzymatic matrix to the electrode surface. To achieve this, the hyperbranched polymer Boltorn H40 (BH40) has been self-assembled at the surface of MWNTs. After the assembling, the suspension of BH40-MWNTs became stable and its functionality was tested by replacing mucin in the enzymatic matrix of a previously reported sandwich-type lactate biosensor. The inclusion of BH40-MWNTs in the biosensor: increased the diffusion coefficient of soluble species by decreasing the elastic properties of the enzymatic matrix, kept the characteristics of the microenvironment where the enzyme is stored, and wired the enzymatic matrix through a 13 μm thick polycarbonate membrane to the electrode surface. It is important to understand that the superstructure of BH40-MWNTs does not increase the active surface of the electrode. Instead of this, it is a conductive 3D network that connects the enzymatic matrix to the electrode. As a result, the response-time of this novel sandwich-type lactate biosensor is much shorter than that of conventional biosensors because the mediator of the enzyme (oxygen) can be regenerated at the enzymatic matrix and it does not have to diffuse to the electrode surface.

1. Introduction

From their discovery, multi-walled and single-walled carbon nanotubes (MWNTs and SWNTs, respectively) have attracted enormous interest due to their unique structural, mechanical and electronic properties [1–4]. These characteristics include high chemical and thermal stability, high elasticity, high tensile strength, and particularly high conductivity [1,2]. The conductivity along with their small size has seen them touted as one of the key materials to be used as molecular wires in molecular electronics [2,4]. Unfortunately, this kind of nanostructures is insoluble in all solvents and most of their promising practical applications are considered to be hindered until the development of a reliable dissolving strategy [4]. In this regard, covalent and non-covalent strategies have been used to disperse MWNTs and SWNTs obtaining results with diverse degrees of success [5–7]. Curiously, most applications involve the deposition of dispersed nanotubes on a surface [4,8]. This step restores the 2D structure where the further electric or electrochemical processes are expected to take place. As a result of the deposition process, most of the 3D capability of carbon nanotubes arrangements is lost [9,10].

In electrochemistry, a 3D mesh of carbon nanotubes would represent a novel kind of electrode where the electrode surface is electrically connected to a region that is some micrometers far from the surface. For the case of hydrogel based biosensors, this property gives the possibility for minimizing the distance where the diffusion of electroactive species is required as well as the chance for establishing direct electron transfer between the enzyme and the electrode surface [11–13]. Both characteristics are important when sandwich type biosensors are considered, since the response-time is a significant drawback of this kind of sensors [14–17].

It is well-known that the performance of enzymatic biosensors is dramatically affected by the physicochemical characteristics of the microenvironment that surrounds the enzyme [18]. The observed activity and stability of the enzyme, as well as the response-time of the sensor are the outcome of the immobilization process and of

* Corresponding author.
E-mail address: fgaray@fcq.unc.edu.ar (M.C. Strumia).

http://dx.doi.org/10.1016/j.snb.2017.01.011
0925-4005/

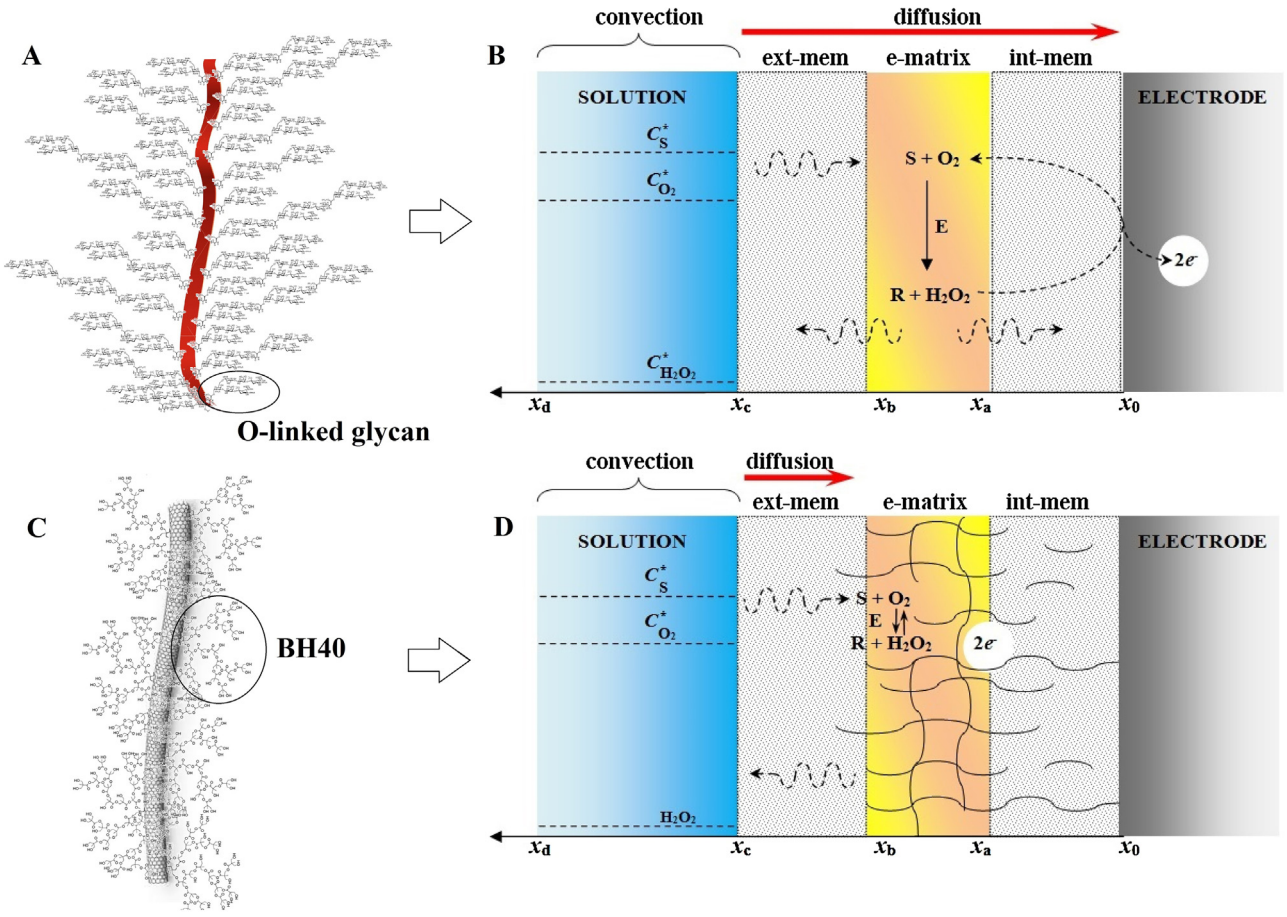

Fig. 1. Schemes of (A) the structure of mucin, (B) the structure of BH40-MWNTs, (C) a conventional sandwich-type amperometric biosensor and (D) a sandwich-type amperometric biosensor wired with the self-assembled structure of BH40-MWNTs.

the electrode material selected for building the sensor. Usually, the stability of these biomolecules is increased when they are in contact with molecules presenting glycosidic groups [19]. Recently, mucin, a glycoprotein with high molecular weight (2×10^6 Da) and extremely long chain (around 2 μm) has been successfully used to prepare lactate and glucose biosensors, see Fig. 1A [16,17,20–22]. Mucin is produced and secreted by mucous cell walls in the digestive tract and it basically has a protein skeleton surrounded by glycosidic branches [16]. The interaction of those branches restricts the conformational arrangement of mucin backbone. As a result, mucin is characterized by an outstretched structure that can achieve 1 μm long [16].

The possibility for arranging a set of molecules in order to get a self-assembled structure that emulates the one of mucin was studied and presented in this manuscript. To achieve this, the hyperbranched polymer Boltorn® H40 (BH40) was self-assembled at the surface of MWNTs. BH40 is a hyperbranched polyester with several hydroxyl groups that has been used to develop biosensors and controlled drug release systems, see Fig. 1C [23,24]. It has been demonstrated that the presence of well-defined polymer brushes on various types of substrates is necessary to improve the performance of the immobilized active agent, which is really important when enzymes are the active compounds incorporated [25]. This hydrophilic environment provides the encapsulation of the enzyme with a higher degree of conformational freedom ensuring its stability and activity. After the assembling, BH40-MWNTs became soluble and its functionality was tested by replacing mucin in an enzymatic matrix composed by lactate oxidase (LOD), mucin and bovine serum albumin (BSA) crosslinked with glutaraldehyde (GTA), see Fig. 1B. That matrix provides a proper environment for the stability and activity of LOD in a sandwich-type lactate biosensor [16,17]. The inclusion of BH40-MWNTs in the biosensor would provide an environment where the enzyme is surrounded by the hydrophilic chains of BH40 that remain its stability, see Fig. 1D.

In this manuscript MWNTs are successfully dispersed and suspended in presence of the hyperbranched polymer BH40. Then, the complex BH40-MWNTs is used for replacing mucin in the enzymatic matrix of a sandwich-type lactate biosensor. The inclusion of BH40-MWNTs did not only improve the viscoelastic properties of the membrane, but also developed a conductive 3D network where the mediator of the enzyme can be regenerated without diffusing to the electrode.

2. Experimental

2.1. Reagents

The MWNTs employed in this work were supplied by Sunnano, China. The nanotubes were synthesized by chemical vapor deposition (CVD) and have around 80% of purity. The diameter ranges between 10 and 30 nm. Boltorn H40 was provided by Perstorp Polyols, Inc., USA (64 hydroxyl groups per molecule and MW of 2833) and used without purification.

All solutions were prepared with deionized (DI) water (18MΩcm) from a Millipore Milli-Q system. The buffer solution (0.1 M) consisted in 0.05 M HK_2PO_4/0.05 M H_2KPO_4 (Merck, Germany). This solution was renewed weekly and small amounts of H_2SO_4 (Baker, USA) or KOH (Merck, Germany) were used to

fix it at pH 7.0. Stock solutions of 0.1 M lactate (Sigma, USA) and 1.5% (v/v) glutaraldehyde (GTA) (Sigma, USA) were prepared in the buffer solution. Lactate oxidase (LOD) (50 U) from Pediococus species (Sigma, USA) was dissolved in 1000 μL of buffer. After dissolution, aliquots of 20 μL of enzyme were separated into 50 vials and stored at −20 °C. Thus, every aliquot bears 1U of LOD. Mucin (Sigma, USA) was powdered and saved as a dry powder at 4 °C. Bovine serum albumin (BSA) (Sigma, USA) was used as received. All solutions were stored at 4 °C. Polycarbonate membranes of 0.05 μm pore size (Millipore, USA) were cut in discs of 6 mm diameter. A Corning syringe filter of Ø = 15 mm (Sigma, USA) modified with a polycarbonate membrane of 0.05 μm pore size was used for filtering the supernatant of BH40-MWNTs.

2.2. Equipment

Fourier Transform Infrared (FT-IR) spectra were obtained on Nicolet 5-SXC FT-IR spectrometer (USA) on AgBr discs. A rotational rheometer Anton Paar Physica MCR 301 (USA) was used to perform the rheological assays. The UV–vis spectra were recorded with a Shimadzu recording spectrophotometer UV-260 (USA). Nuclear magnetic resonance studies (^{1}H NMR) in DMSO-d_6 were obtained on Bruker Avance II, 400.16 MHz (USA) with inverse detection probe. The samples were centrifuged with a Rolco model CM-2050 centrifuge (Argentina).

Electrochemical experiments were performed with an Autolab PGSTAT30 Electrochemical Analyzer (Eco Chemie, Netherlands). The measurements were carried out using a conventional three-electrode system with a Pt wire as the counter electrode, Ag|AgCl|KCl (3 M) (CH instruments, USA) was the reference electrode, and a 2 mm diameter Pt disc (CH instruments, USA) was the working electrode. Amperometric detection was obtained under batch conditions with stirring of 120 rpm during the whole electrochemical experiment.

Transmission electron microscopy (TEM) observation of the composite was performed with a JEOL 100 CX II TEM (USA) operated under an acceleration voltage of 100 kV (PLAPIQUI, Bahía Blanca).

2.3. Preparation of BH40-MWNTs dispersion

An aliquot of 10 mg MWNTs was suspended in 1.0 mL DMSO and homogenized in an ultrasonic bath for 40 min. Then, 200 mg of BH40 was added to the MWNTs suspension, and the mixture was newly sonicated until complete dispersion of the beads of BH40. After this step, the dispersion was heated at 70 °C until achieve a constant mass value due to the solvent evaporation. The resulting black film was redispersed in 10 mL of DI water and the mixture was racked in a tube and centrifuged at 9000 rpm for 20 min. As a result, two phases were obtained. The precipitated fraction was dried in a vacuum oven for 24 h and the gravimetric assay provided a mass of 9.2 mg. The other fraction consisted on 1.5 mL of a dark supernatant that was collected and filtered with a syringe filter in which a 50 nm pore size polycarbonate membrane was placed. In practice, all MWNTs passed through the filter and a final volume of 1.48 mL was recovered. The concentration of BH40-MWNTs was estimated in 540 mg L^{-1}. No precipitated fraction was observed from this dispersion of MWNTs after several months of preparation.

2.4. Preparation of samples for FTIR measurements

FTIR spectroscopy was used to study the chemical groups in samples of GTA, BH40, and in a mixture of both reagents. FTIR spectra of the mixture were measured at 1, 10, 20 and 30 min after the first contact of the reagents.

The samples consisted on: (1) a drop of 10 μL of 1.5% (v/v) GTA in DI water and placed on the surface of a disk of AgBr; (2) a sample of 1.0 mg of BH40 dissolved in a drop of 10 μL of DI water and (3) a sample of 1.0 mg of BH40 dissolved in a drop of 10 μL GTA diluted to 1.5% v/v in DI water and then spread out on the surface of a AgBr disk.

2.5. Preparation of samples for rheological experiments

The sample of BSA consisted on 50.0 mg of BSA diluted into 500 μL of DI water and then mixed for 3 min. The BSA-BH40 mixture was prepared with 25.0 mg of BSA and 25.0 mg of BH40 diluted into 500 μL of DI water and mixed for 3 min. The BSA-BH40-MWNTs was prepared with 25.0 mg of BSA mixed with 250 μL of the BH40-MWNTs water dispersion in a 1.5 mL vial and sonicated for 10 s. After this step, 250 μL of DI water are added and subsequently mixed for 3 min. All systems (BSA; BSA-BH40 and BSA-BH40-MWNTs) were crosslinked by adding 250 μL of 1.5% (v/v) GTA to each vial. A 25 mm diameter plate–plate geometry with 1.5 mm plate separation was used. Once the products were cured, rheological assays were performed with 1% of deformation to ensure that the experiments are performed in the linear viscoelastic region (LVR).

2.6. Preparation of the sample for TEM measurements

The sample of BSA-BH40-MWNTs was prepared by mixing 50.0 mg of BSA with 500 μL of the BH40-MWNTs water dispersion in a 1.5 mL vial and sonicated for 30 s. After this step, 500 μL of DI water was added and the resulting suspension was mixed for 3 min. Before measurement, the sample was sonicated for 30 s and two drops of the suspension were placed on a Formwar film supported by a 200-mesh copper grid.

2.7. Preparation of LOD-BSA-BH40-MWNTs

In order to prepare the matrix of LOD-BSA-BH40-MWNTs, 3.0 mg of BSA was mixed with 30 μL of the MWNTs water dispersion in a 0.3 mL vial and then sonicated for 10 s. After this step, 20 μL of DI water and 10 μL of 1 U LOD were added and then mixed for 3 min. An aliquot of 6 μL of this mixture was placed over a polycarbonate disc and crosslinked using 3 μL of 1.5% (v/v) GTA. Finally, a second polycarbonate disc was used to cover the enzymatic matrix and the sandwich-type amperometric biosensor assembled as previously described [16,17]. The biosensor is washed with the buffer solution for 5 min after the addition of GTA.

2.8. Preparation of LOD-BSA-mucin

A mixture composed by 4.2 mg mucin and 1.8 mg BSA was dissolved in 40 μL of buffer solution. The proteins were mixed for 3 min until a colloidal suspension was obtained and then transferred to a vial containing 20 μL of 1U LOD. The resulting suspension of LOD-BSA-mucin (60 μL) was then mixed for 3 min and stored at 4 °C.

To prepare the enzymatic electrode, aliquots of 6 μL of the LOD-BSA-mucin mixture and 3 μL of 1.5% (v/v) GTA were mixed and finally entrapped between two membranes of polycarbonate following the same protocol described for the matrix of LOD-BSA-BH40-MWNTs.

3. Results and discussion

3.1. Characterization of BH40-MWNTs structure

When MWNTs are sonicated in presence of the hyperbranched polymer BH40, a dispersion of MWNTs is obtained. This dispersion is very stable since no precipitated fraction is observed after

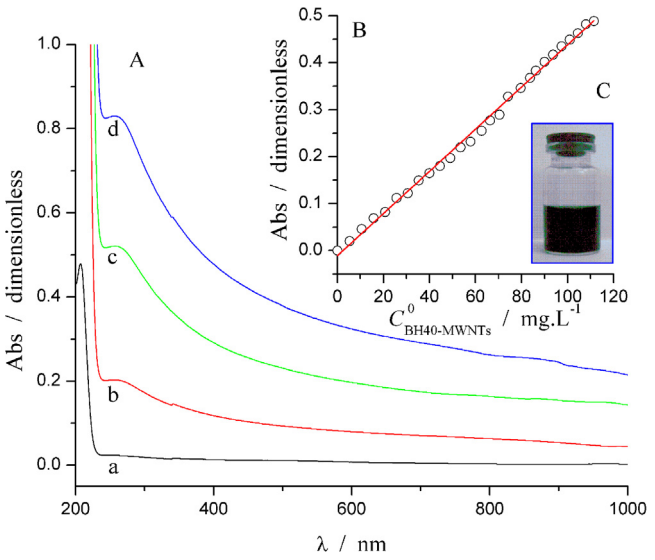

Fig. 2. (A) UV–vis spectra corresponding to aqueous dispersions of BH40 (a) and to aqueous dispersions of BH40-MWNTs/mg L^{-1}: 26 (b), 58 (c), and 86 (d). The concentration values are refferred to the total concentration (C^0). (B) Calibration curve for the absorbance (Abs) at 500 nm of different concentrations of BH40-MWNTs. (C) Photograph of 540 mg L^{-1} BH40-MWNTs dispersion.

several months of preparation (see Section 2.3 for details). The characterization of this self-assembled structure is performed by UV–vis and ^{1}H NMR. It is considered that bundled carbon nanotubes should not absorb in the UV–vis region and so, single carbon nanotubes should be the unique absorbing species in this region [26,27]. Fig. 2A shows UV–vis spectra of BH40-MWNTs dispersed in aqueous media. The absorption band at 260 nm has been assigned to the π-π* transition of the aromatic rings of nanotubes. This absorption band extends above 1000 nm. However, it is considered that the absorbance at 500 nm is not affected by the environment of the nanotubes [28–31]. Accordingly, the extinction coefficient of single carbon nanotubes at 500 nm, $\varepsilon_{500} = 28.6\ cm^2\ mg^{-1}$, is used to determine the percentage of single MWNTs of the dispersion [29]. The slope of the linear regression is $Q_{500} = (4.49 \pm 0.05)\ cm^2\ mg^{-1}$, pointing out the presence of 15.7% of single MWNTs.

Considering that the mother solution should have a total concentration of BH40-MWNTs (C^0) of 540 mg L^{-1}, UV–vis data would indicate that the actual concentration of single MWNTs is 84.8 mg L^{-1}. The rest of MWNTs should be dispersed in the bundled form, since no precipitated fraction was observed in the mother solution after several months of preparation.

Molecular interactions and electronic properties of BH40-MWNTs were studied by NMR [32]. This technique has been widely used for studying host-guest interactions between organic molecules such as cyclodextrins, calixarenes and more recently with carbon nanotubes [32–35]. Even thought MWNTs do not have hydrogen, the aqueous dispersions of MWNTs are stabilized by the presence of BH40 and it is expected to find shifts on the NMR response due to the molecular interaction of these species. In this regard, the microstructure of BH40 has been fully characterized by ^{1}H NMR [36–38]. Fig. 3 shows the ^{1}H NMR spectra corresponding to (a) 500 μL of HB40 20 mg mL^{-1} and (b) the system obtained 72 h after the addition of 20 μL of 1 mg mL^{-1} MWNTs to the solution (a). The measurements were performed in DMSO-d_6. The most relevant signals of BH40 can be summarized as linear units (δ = 4.93 ppm, $CH_2O\underline{H}$), terminal units (δ = 4.61 ppm, $CH_2O\underline{H}$), dendritic units (δ = 4.20 ppm, $C\underline{H}_2OR$) and CH_2OH groups of terminal units (δ = 3.50 ppm). Other signals related to —CH_3 groups and molecules of solvent have been indicated in Fig. 3.

The presence of MWNTs causes downfield shift, in 0.02 and 0.03 ppm, of the signals of hydroxyl groups of terminal and linear units. On the other side, hydrogen signals of methylene groups, CH_2OR and $C\underline{H}_2OH$, are shifted towards upfield. This behavior would indicate the hydrophobic interaction of methylene units with MWNTs, while the hydroxyl groups are exposed to the solution [37]. A scheme of BH40 molecule can be found in the Supporting Information as Fig. S-1.

3.2. Analysis of the crosslinking reaction of BH40

FTIR was used to check the efficiency of crosslink reactions between GTA and BH40. Fig. 4A shows a set of FTIR spectra corresponding to the stretching bands of CH bonds detected between 3000 and 2600 cm^{-1}. Alkane CH bonds are fairly ubiquitous and considered to be less useful for determining the structure. However, in this region the CH bond of aldehyde groups have a typical stretching band at 2868 cm^{-1}, while the stretching of CH groups of BH40 shows a maximum at 2885 cm^{-1}. During the crosslinking of BH40 with GTA, aldehyde groups are consumed to produce acetal and hemiacetal bridges [39–41]. Consequently, it is observed that the absorption peak at 2868 cm^{-1}, relatively decreases during the 30 min of reaction while the stretching of CH groups of BH40 prevails after this time. The analysis of the ratio between both peaks indicates that most aldehyde groups of GTA would have reacted after being exposed to BH40 for 30 min, Fig. 4D.

The signal of CO stretching corresponding to aldehyde group appears at 1720 cm^{-1} while the one of ester groups has a peak of absorption at 1740 cm^{-1} [38,39]. Since these signals are very close they have been marked with arrows in Fig. 4B. The signal at 1726 cm^{-1} has been assigned to GTA molecules while the one at 1741 cm^{-1} corresponds to the CO stretching of the BH40 ester groups. The relative diminution of the signal at 1726 cm^{-1} with regards to the one at 1741 cm^{-1} indicates that GTA molecules are consumed to produce acetal and hemiacetal bridges, while the ester groups do not react under these conditions. Fig. 4B shows also a peak at 1645 cm^{-1} corresponding to the bending of water molecules, which is the solvent of glutaraldehyde. The height of this peak decreases due to the evaporation of water during the 30 min of the experiment, curves 4 B (b–e).

The formation of the ether groups that constitute the acetal and hemiacetal bridges can be observed from Fig. 4C, where the relative increment of the absorption bands at 1126 and 965 cm^{-1} is evident during 30 min of reaction. Those bands have been assigned to the asymmetric and symmetric stretching of COC groups [40]. Fig. 4E shows the ratio of the signal at 1126 cm^{-1} for different times of the crosslinking reaction. These results would indicate that the crosslinking reaction of BH40 with GTA involves the formation of acetal and hemiacetal bridges. These bridges transform the solution of BH40 into a hydrogel-like product after 4 or 5 min of reaction. Regardless the black color that characterizes systems with carbon nanotubes, similar outcome has been observed for the samples in which BH40 stabilizes the dispersion of MWNTs. Unfortunately, it was not possible to obtain reliable FTIR spectra from systems containing nanotubes.

3.3. Characterization of BSA-BH40-MWNTs matrix

A TEM image of the distribution of MWNTs within a BSA-BH40-MWNTs matrix is shown in Fig. 5. As it can be observed, the dispersion of MWNTs is quite good and the amount of MWNTs arranged in branches is very low, other TEM images can be found in the Supporting Information as Fig. S-2. From the image, it is possible to estimate that the outer diameter of MWNTs is between 10 and 30 nm, which is in agreement with the provider.

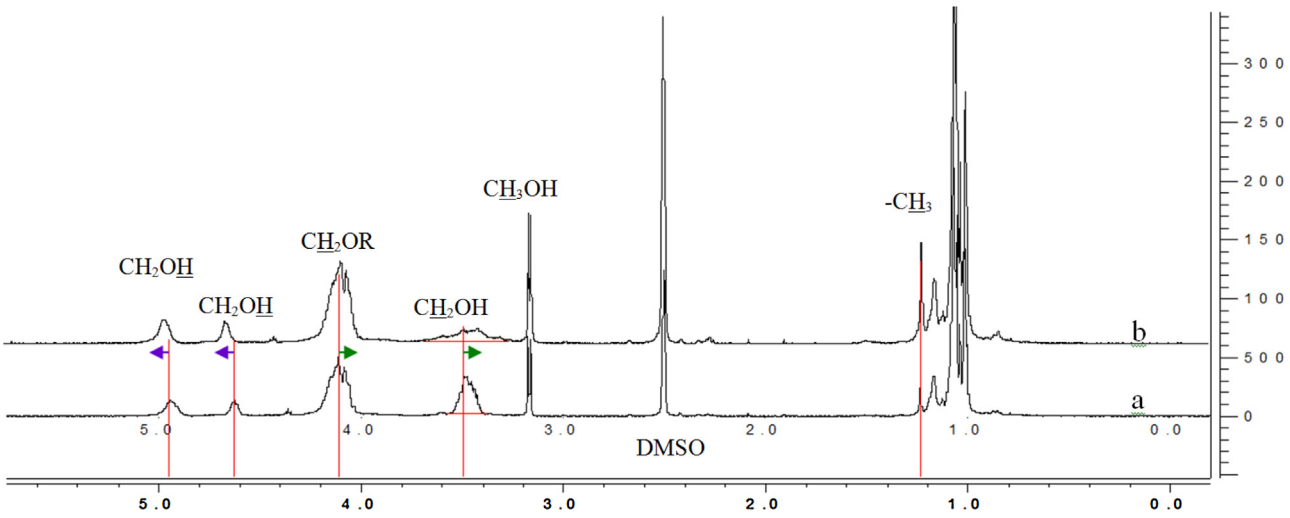

Fig. 3. ^{1}H NMR spectra for: (a) 20 mg mL^{-1} BH40 dissolved in 500 μL DMSO-d_6 and (b) 72 h after the addition of 20 μL of 1 mg mL^{-1} MWNTs to solution (a).

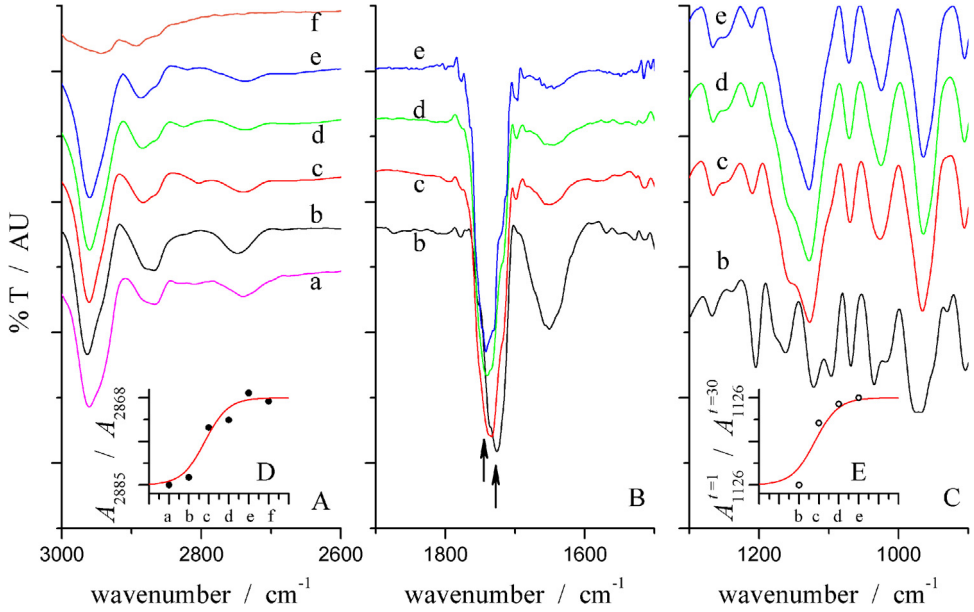

Fig. 4. (A–C) different regions of FTIR spectra for (a) 0.15 mg GTA, 1.0 mg BH40 + 0.15 mg GTA after (b) 1 min, (c) 10 min, (d) 20 min, (e) 30 min, and (f) 1.0 mg BH40. The samples were aqueous solutions dried on the surface of AgBr disks. (D) Normalized ratio between the Abs of signals observed at 2885 and 2868 cm^{-1}. (E) Normalized ratio between the Abs of the signal observed at 1126 cm^{-1} from 1 to 30 min.

Rheological measurements allow the evaluation of viscoelasticity of diverse composites, hydrogels, or polymeric matrixes as a function of their composition. In the case of a hydrogel that has to immobilize an enzyme, the viscoelasticity of the enzymatic matrix is a relevant parameter that influences the activity of the enzyme. All systems were crosslinked with 1.5% (v/v) GTA, just before starting the experiment.

Fig. 6 shows the dependence of the elastic (G') and viscous (G") moduli on frequency (**ω**) for hydrogels prepared from BSA, BSA-BH40 and BSA-BH40-MWNTs. All systems were crosslinked with 1.5% (v/v) GTA and cured for 30 min. The low variability observed for **ω** < 10 Hz is characteristic of covalently crosslinked networks [42]. Above 10 Hz both viscoelastic parameters increase pointing out higher rigidness of all products for those frequencies.

The hydrogel prepared with BSA and BH40 exhibits higher values of G' and G" moduli than that prepared only with BSA. This behavior would indicate that the mixture BSA-BH40 is crosslinked by GTA more efficiently than the hydrogel from BSA. In this regard, it should be considered that BSA has only 19 lysine groups available for reacting with GTA whereas, as it was concluded from the analysis of FTIR spectra, BH40 has around 30 OH groups that could react in presence of GTA [43]. Moreover, BH40 should react faster and eventually more efficiently than BSA since the former is smaller and more flexible than the latter. The mobility and flexibility of BH40 is compromised when it is attached to MWNTs. As a result, the moduli of viscoelastic parameters diminish for the matrix with BH40 and MWNTs. The hydrophobic interaction observed by ^{1}H NMR between the methylene units of BH40 and MWNTs would not only favor the dispersion of MWNTs, but also it would reduce the mobility of BH40 and its capacity for crosslinking with other molecules. Moreover, electroactive species such as H_2O_2 would be able to react electrochemically at the ends of MWNTs if they are properly wired to the electrode surface.

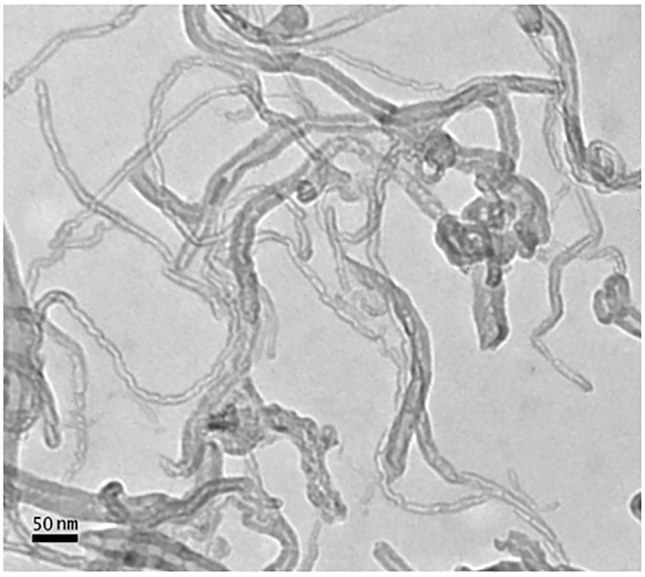

Fig. 5. TEM image of the BSA-BH40-MWNTs system.

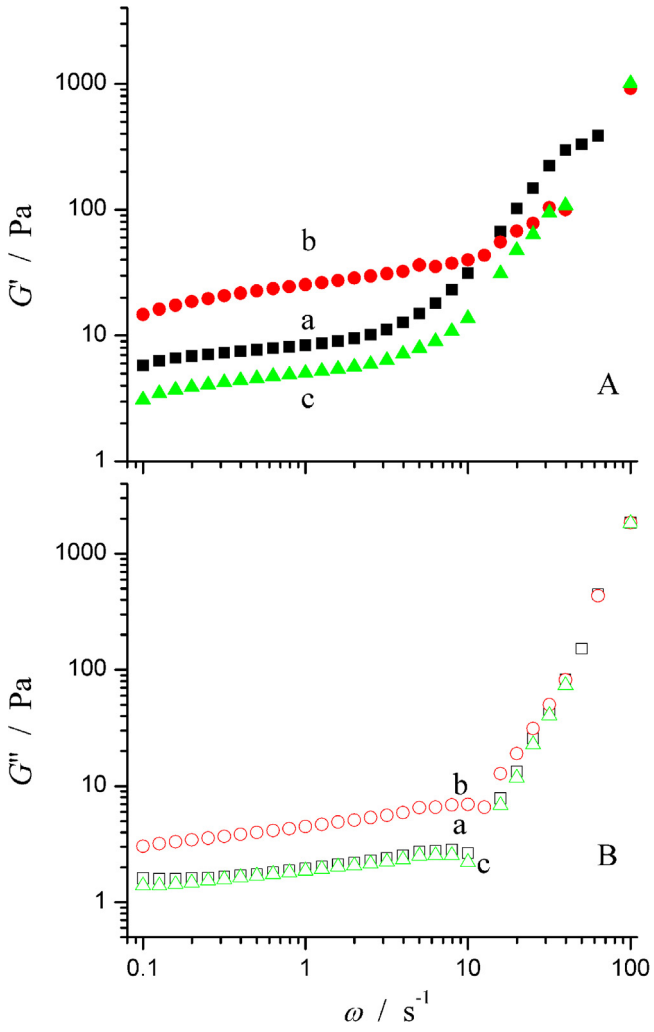

Fig. 6. Dependence of (A) elastic and (B) viscous moduli of BSA (a), BSA-BH40 (b) and BSA-BH40-MWNTs (c) as functions of frequency. Data obtained at pH 7.0 and 20 °C.

3.4. Chronoamperometric response of the biosensor prepared with LOD-BSA-BH40-MWNTs

Lactate is an anionic product formed from the oxidation of pyruvate during anaerobic glucose metabolism. The quantification of L-lactate by amperometric biosensors is important for clinical purposes, athletic performance, and processing industries [17]. Lactate oxidase (LOD) catalyzes the oxidation of lactate to pyruvate. In presence of dissolved O_2, the enzyme can be reoxidized releasing H_2O_2. This last product can be re-oxidized at the electrode and the current is proportional to the amount of dissolved lactate. The electrochemical reaction also restores the former concentration of O_2 into the inner membrane and it diffuses to the enzymatic matrix [17]. LOD is a rather weak enzyme that can be easily denatured. As a consequence, it is usually observed that its catalytic properties quickly decay once it is removed from a natural matrix [16].

The performance of a LOD-sensor prepared with 0.1U of LOD crosslinked with GTA within a BSA-BH40-MWNTs hydrogel is exhibited in Fig. 7. Fig. 7A shows how the chronoamperometric response evolves after successive additions of a standard solution of lactate while Fig. 7B presents the linear dependence between the steady-state current and lactate concentration. The current corresponds to the oxidation of the enzymatic product H_2O_2 at 0.65 V. The slope calculated from the data of Fig. 7B is (0.28 ± 0.01) mA M^{-1}, which is similar to the sensitivity expected for an equivalent sensor, but prepared with a 30/70 mass ratio of BSA/mucin (0.34 ± 0.05) mA M^{-1} [20]. It is well-known that the sensitivity is a key parameter that might condition the detection limit of a sensor. However, it is also important to consider other parameters such as the linear range and the response-time of the biosensor. In previous works, the composition of a LOD-BSA-mucin biosensor was optimized and its response simulated with a numerical model [16,20,21]. Its response is now compared with the enzymatic matrix LOD-BSA-BH40-MWNTs. Sandwich-type biosensors usually require a conditioning time before performing the first measurement. The LOD-BSA-BH40-MWNTs biosensor required 1500 s at 0.65 V to obtain a proper base line. The standard deviation calculated from data collected during the last 300 s of this conditioning time was used to calculate the blank signal providing a limit of detection equal to 0.9 μM. The linear response is considered to extend up to 1.5 mM of lactate. The coefficient of determination $r^2 > 0.9991$ within the selected linear range, Fig. 7B. These parameters are similar to those of a LOD-BSA-mucin biosensor. However, the LOD-BSA-BH40-MWNTs biosensor required only 7 s for reaching 95% of the value of limiting current, whereas an equivalent biosensor based on a LOD-BSA-mucin hydrogel showed a response-time of 80 s, Fig. 7C [16,20,21].

The remarkable improvement on the response-time of the new sensor was an unexpected behavior, since it cannot be explained by considering the diverse difusional processes related to the enzymatic catalysis [20,21]. When the enzymatic hydrogel and the polycarbonate membranes were placed together to prepare a conventional sandwich-type biosensor, they have a thickness estimated as (30 ± 4) μm [20,21]. In this regard, it is necessary to consider that the substrate and the enzymatic products have to diffuse through the whole biosensor, see the red arrow of Fig. 1C. Calculations performed specifically for this kind of system are consistent with the need of around 80 s to achieve the steady-state of the chronoamperometric response [20,21].

To explain the speed of response of LOD-BSA-BH40-MWNTs biosensor, a different hypothesis is required. Also, it is necessary to remember that the suspension of BH40-MWNTs can pass through the pores of polycarbonate, since it was already filtered through this membrane, see Materials and Methods. First, it has to be assumed that one or more pores of polycarbonate membranes are filled with MWNTs. Second it is necessary to consider that,

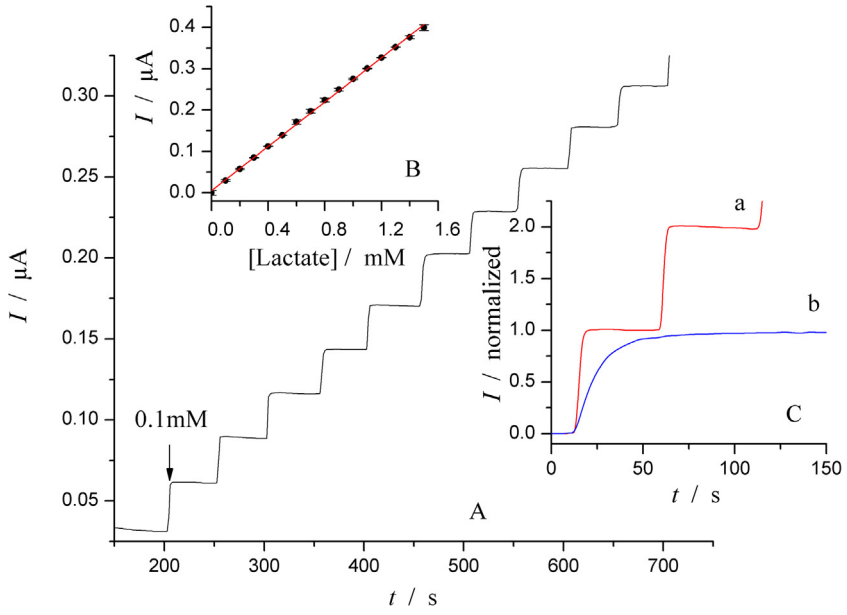

Fig. 7. (A) Current–time curve for a biosensor prepared with 0.1 U of LOD crosslinked with GTA within a BSA-BH40-MWNTs hydrogel upon successive additions from a lactate standard solution. (B) Calibration curve prepared from the steady-state currents of figure A. (C) Comparison of the normalized transients of LOD-sensors prepared with BSA-BH40-MWNTs (a) and BSA-mucin (b). Both systems were crosslinked for 5 min with 3 μL of GTA 1.5% v/v. In all cases, every addition of lactate increased the bulk concentration in 0.1 mM and the current corresponds to the oxidation of H_2O_2 at 0.65 V.

for the case of the inner membrane, the MWNTs could wire the network of MWNTs dispersed into the enzymatic matrix with the electrode surface. As a result of these two assumptions it is possible to expect that H_2O_2 does not have to diffuse through the enzymatic matrix and the inner polycarbonate membrane for reacting electrochemically. Instead of this, might be oxidized at the edges of MWNTs that are inside the enzymatic matrix. In addition, the concentration of O_2 would remain as a constant since it would regenerate at the enzymatic matrix. Also, the substrate would only have to diffuse through the outer polycarbonate membrane, see the red arrow of Fig. 1D. All these considerations are consistent with the remarkable response-time observed for the sandwich-type amperometric biosensor wired with the self-assembled structure of BH40-MWNTs.

4. Conclusions

In this work, MWNTs have been successfully suspended into a water solution of the hyperbranched BH40 polymer. The BH40-MWNTs can be considered as a self-assembled structure that forms stable suspensions in water. The structure was characterized and then used for constructing a 3D MWNTs scaffold into a hydrogel based biosensor. The biosensor consisted on an enzymatic matrix where the enzyme LOD is crosslinked with GTA in presence of BSA and a dispersion of MWNTs-BH40. The novel biosensor significantly reduced the response-time with respect to a biosensor prepared with LOD-BSA-mucin. The speed of response of the biosensor cannot be explained by considering the usual diffusion of reagents and products [20,21]. It is assumed that the mesh of MWNTs is wired to the electrode surface allowing the re-oxidation of H_2O_2 at the enzymatic matrix. Thus, the ends of MWNTs can be close to the enzymes, providing a biosensor of first kind where the mediator O_2 is regenerated from H_2O_2 into the enzymatic matrix. From the analytical point of view, the new sandwich-type enzymatic biosensor keeps the remarkable characteristics of a previous developed biosensor [16,17] and improves the response-time from 80 to 7 s.

Acknowledgments

This work was funded by PIP CONICET No. 112-20110101029, FONCYT-PICT-2011-0654 and Secyt-UNC Res. 203/14 and 162/14. M.R. Romero, C.I. Alvarez Igarzabal, A.M. Baruzzi, M.C. Strumia and F. Garay are research fellows of CONICET.

Appendix A. Supplementary data

Supplementary data associated with this article can be found, in the online version, at http://dx.doi.org/10.1016/j.snb.2017.01.011.

References

[1] E.V. Barrera, M.L. Shofner, E.L. Corral, in: M. Meyyappan (Ed.), Carbon Nanotubes: Science and Applications, CRC Press, Boca Raton, FL, 2004, pp. 253–276.
[2] H. Peng, Q. Li, in: T. Chen (Ed.), Industrial Applications of Carbon Nanotubes, Elsevier Inc, Amsterdam, 2017, pp. 47–150.
[3] P.P. Mercè, in: M.J. Esplandiu Egido, M.V. Zafra (Eds.), Carbon Nanotubes as Platforms for Biosensors with Electrochemical and Electronic Transduction, Springer, Heidelberg, Germany, 2012, pp. 1–78.
[4] Z. Zhu, L. Garcia-Gancedo, A.J. Flewitt, H. Xie, F. Moussy, W.I. Milne, A critical review of glucose biosensors based on carbon nanomaterials: carbon nanotubes and graphene, Sensors 12 (2012) 5996–6022.
[5] D. Yang, X. Zhang, C. Wang, Y. Tang, J. Li, J. Hu, Preparation of water-soluble multi-walled carbon nanotubes by Ce(IV)-induced redox radical polymerization, Prog. Nat. Sci. 19 (2009) 991–996.
[6] M. Eguílaz, A. Gutierrez, G.A. Rivas, Non-covalent functionalization of multi-walled carbon nanotubes with cytochrome c: enhanced direct electron transfer and analytical applications, Sens. Actuators B Chem. 225 (2015) 74–80.
[7] C. Hu, X. Chen, S. Hu, Water-soluble single-walled carbon nanotubes films: preparation, characterization and applications as electrochemical sensing films, J. Electroanal. Chem. 586 (2006) 77–85.
[8] B.R. Adhikari, M. Govindhan, A. Chen, Carbon nanomaterials based electrochemical sensors/biosensors for the sensitive detection of pharmaceutical and biological compounds, Sensors 15 (2015) 22490–22508.
[9] Z. Dai, L. Liu, X. Qi, J. Kuang, Y. Wei, H. Zhu, Z. Zhang, Three-dimensional sponges with super mechanical stability: harnessing true elasticity of individual carbon nanotubes in macroscopic architectures, Sci. Rep. 6 (2016) 18930.
[10] S. Ahadian, J. Ramón-Azcón, M. Estili, X. Liang, S. Ostrovidov, H. Shiku, M. Ramalingam, K. Nakajima, Y. Sakka, H. Bae, T. Matsue, A. Khademhosseini, Hybrid hydrogels containing vertically aligned carbon nanotubes with

anisotropic electrical conductivity for muscle myofiber fabrication, Sci. Rep. 4 (2014) 4271.
[11] D. Zhai, B. Liu, Y. Shi, L. Pan, Y. Wang, W. Li, R. Zhang, G. Yu, Glucose sensor based on Pt nanoparticle/polyaniline hydrogel heterostructures, ACS Nano 7 (2013) 3540–3546.
[12] M. Zhou, S. Dong, Bioelectrochemical interface engineering: toward the fabrication of electrochemical biosensors, biofuel cells, and self-powered logic biosensors, Acc. Chem. Res. 44 (2011) 1232–1243.
[13] W. Putzbach, N.J. Ronkainen, Immobilization techniques in the fabrication of nanomaterial-based electrochemical biosensors: a review, Sensors 13 (2013) 4811–4840.
[14] R.H. Capra, M.C. Strumia, P.M. Vadgama, A.M. Baruzzi, Mucine/carbopol matrix to immobilize the oxalate oxidase in an urine oxalate biosensor, Anal. Chim. Acta 530 (2005) 49–54.
[15] R.H. Capra, A.M. Baruzzi, L.M. Quinzani, M.C. Strumia, Rheological, dielectric and diffusion analysis of mucin/carbopol matrices used in an amperometric biosensors, Sens. Actuators B Chem. 124 (2007) 466–476.
[16] M.R. Romero, A.M. Baruzzi, F. Garay, Design and optimization of a lactate amperometric biosensor based on lactate oxidase cross-linked with polymeric matrixes, Sens. Actuators B Chem. 131 (2008) 590–595.
[17] M.R. Romero, F. Ahumada, A.M. Baruzzi, F. Garay, Amperometric biosensor for direct blood lactate detection, Anal. Chem. 82 (2010) 5568–5572.
[18] J. Wang, Electrochemical glucose biosensors, Chem. Rev. 108 (2008) 814–825.
[19] M. Zhang, A. Smith, W. Gorski, Carbon nanotube-chitosan system for electrochemical sensing based on dehydrogenase enzymes, Anal. Chem. 76 (2004) 5045–5050.
[20] M.R. Romero, A.M. Baruzzi, F. Garay, Mathematical modeling and experimental results of a sandwich-type amperometric biosensor, Sens. Actuators B Chem. 162 (2012) 284–291.
[21] M.R. Romero, A.M. Baruzzi, F. Garay, How low does the oxygen concentration go within a sandwich-type amperometric biosensor? Sens. Actuators B Chem. 174 (2012) 279–284.
[22] L. Colombo, A.M. Baruzzi, F. Garay, Analysis and optimization of a hydrogel matrix for the development of a sandwich-type glucose biosensor, Sens. Actuators B Chem. 211 (2015) 125–130.
[23] A. Tiwari, S. Aryal, S. Pilla, S. Gong, An amperometric urea biosensor based on covalently immobilized urease on an electrode made of hyperbranched polyester functionalized gold nanoparticles, Talanta 78 (2009) 1401–1407.
[24] S. Chen, X.Z. Zhang, S.X. Cheng, R.X. Zhuo, Z.W. Gu, Functionalized amphiphilic hyperbranched polymers for targeted drug delivery, Biomacromolecules 9 (2008) 2578–2585.
[25] J. Vartiainen, M. Rättö, S. Paulussen, Antimicrobial activity of glucose oxidase-immobilized plasma-activated polypropylene films, Packag. Technol. Sci. 18 (2005) 243–251.
[26] Y. Junrong, N. Grossiord, C.E. Koning, J. Loos, Controlling the dispersion of multi-wall carbon nanotubes in aqueous surfactant solution, Carbon 45 (2007) 618–623.
[27] J.S. Laurent, C. Voisin, G. Cassabois, C. Delalande, P. Roussignol, O. Jost, L. Capes, Ultrafast carrier dynamics in single-wall carbon nanotubes, Phys. Rev. Lett. 90 (2003) 057404.
[28] O.K. Kim, J. Je, J.W. Baldwin, S. Kooi, P.E. Pehrsson, L.J. Buckley, Solubilization of single-wall carbon nanotubes by supramolecular encapsulation of helical amylase, J. Am. Chem. Soc. 125 (2003) 4426–4427.
[29] V.A. Sinani, M.K. Gheith, A.A. Yaroslavov, A.A. Rakhnyanskaya, K. Sun, A.A. Mamedov, J.P. Wicksted, N.A. Kotov, Aqueous dispersions of single-wall and multiwall carbon nanotubes with designed amphiphilic polycations, J. Am. Chem. Soc. 127 (2005) 3463–3472.
[30] R. Rastogi, R. Kaushal, S.K. Tripathi, A.L. Kaur, I. Sharma, L.M. Bharadwaj, Comparative study of carbon nanotube dispersion using surfactants, J. Colloid Interface Sci. 328 (2008) 421–428.
[31] S.J. Henley, R.A. Hatton, G.Y. Chen, C. Gao, H. Zeng, H.W. Kroto, S.R.P. Silva, Enhancement of polymer luminescence by excitation-energy transfer from mufti-walled carbon nanotubes, Small 3 (2007) 1927–1933.
[32] D.J. Nelson, P.T. Perumal, C.N. Brammer, P.S. Nagarajan, Effect of single-walled carbon nanotube association upon representative amides, J. Phys. Chem. C 113 (2009) 17378–17386.
[33] N. Basílio, V. Francisco, L. García-Río, Independent pathway formation of guest-host in host ternary complexes made of ammonium salt, calixarene, and cyclodextrin, J. Org. Chem. 77 (2012) 10764–10772.
[34] J. Szejtli, Introduction and general overview of cyclodextrin chemistry, Chem. Rev. 98 (1998) 1743–1754.
[35] D.J. Nelson, R. Kumar, Characterizing covalently sidewall-functionalized SWNTs, J. Phys. Chem. C 117 (2013) 14812–14823.
[36] E. Žagar, M. Žigon, Characterization of a commercial hyperbranched polyester based on 2,2- bis(methylol propionic)acid, Macromolecules 35 (2002) 9913–9925.
[37] E. Žagar, M. Žigon, Molar mass distribution of a commercial aliphatic hyperbranched polyester based on 2,2-bis(methylol)propionic acid, J. Chromatogr. A 1034 (2004) 77–83.
[38] E. Žagar, M. Husvik, J. Grdadolnik, M. Žigon, A. Zupancic-Valant, Effect of annealing on the rheological and thermal properties of aliphatic hyperbranched polyester based on 2,2-bis(methylol)propionic acid, Macromolecules 38 (2005) 3933–3942.
[39] J. Wu, N. Wang, L. Wang, H. Dong, Y. Zhao, L. Jiang, Unidirectional water-penetration composite fibrous film *via* electrospinning, Soft Matter 8 (2012) 5996–5999.
[40] H. Chen, G. Li, H. Chi, D. Wang, C. Tu, L. Pan, L. Zhu, F. Qiu, F. Guo, X. Zhu, Alendronate-conjugated amphiphilic hyperbranched polymer based on boltorn H40 and poly(ethylene glycol) for bone-targeted drug delivery, Bioconjugate Chem. 23 (2012) 1915–1924.
[41] H.S. Mansur, C.M. Sadahira, A.N. Souza, A.A.P. Mansur, FTIR spectroscopy characterization of poly (vinyl alcohol) hydrogel with different hydrolysis degree and chemically crosslinked with glutaraldehyde, Mater. Sci. Eng. C 28 (2008) 539–548.
[42] C.P. Broedersz, K.E. Kasza, L.M. Jawerth, S. Münster, D.A. Weitz, F.C. MacKintosh, Measurement of nonlinear rheology of cross-linked biopolymer gels, Soft Matter 6 (2010) 4120–4127.
[43] B.X. Huanga, H.Y. Kima, C. Dass, Probing three-dimensional structure of bovine serum albumin by chemical cross-linking and mass spectrometry, J. Am. Soc. Mass Spectrom. 15 (2004) 1237–1247.

Biographies

Marcelo Ricardo Romero, Doctor (Universidad Nacional de Córdoba, 2011). Currently he is assistant professor at the Department of Organic Chemistry, School of Chemical Science, National University of Córdoba and Research Fellow of CONICET, Argentina. His fields of interest include electrochemistry, analytical chemistry, polymer science, electronic devices and biosensors.

Damian Oscar Peralta, Doctor (Universidad Nacional de Río Cuarto, 2010). Currently he is support staff of CONICET, Argentina. His fields of interest include pollution assessment, analysis and speciation of microcystins using voltammetric and spectrometric techniques.

Cecilia Inés Alvarez Igarzabal, Doctor (Universidad Nacional de Córdoba, 1993). Currently she is full Professor at the Department of Organic Chemistry, School of Chemical Science, Universidad Nacional de Córdoba and Research Fellow of CONICET, Argentina. Her fields of interest include synthesis, characterization and application of new polymeric materials and polymer science.

Ana María Baruzzi, Doctor (Universidad Nacional de Córdoba, 1981). Currently she is full professor at the Department of Physical Chemistry, School of Chemical Science, National University of Córdoba and Research Fellow of CONICET, Argentina. Her fields of interest include electrochemistry, analytical chemistry, polymer science and biosensors.

Miriam Cristina Strumia, Doctor (Universidad Nacional de Córdoba, 1982). Currently she is full professor at the Department of Organic Chemistry, School of Chemical Science, National University of Córdoba and Researcher of CONICET, Argentina. Her fields of interest include the synthesis of new nanostructured materials from polymers and dendritic molecules: physicochemical characterization and application.

Fernando Sebastián Garay, Doctor (Universidad Nacional de Córdoba, 2002). Currently he is adjunct professor at the Department of Physical Chemistry, School of Chemical Science, National University of Córdoba and Researcher of CONICET, Argentina. His fields of interest include electrochemistry, numerical and digital simulations, analytical chemistry, in situ techniques, polymer science and biosensors.